HOT-ELECTRON NOISE IN HEMT CHANNELS AND OTHER 2-DEG STRUCTURES

Arvydas Matulionis

Semiconductor Physics Institute, A. Goštauto 11, 2600 Vilnius, Lithuania

A review of experimental results on microwave hot-electron noise specific to two-dimensional electron gas channels is given. Variation of electric field strength, heterobarrier height, doping and electron density, channel length, lattice temperature, microwave frequency have been used to excite/quench hot-electron velocity fluctuations of different origin. The noise sources specific to zero-heterojunction (planar-doped), single-, double- and triple-heterojunction channels are analyzed in terms of fast intrawell and interwell kinetic processes.

Introduction

Modern heterostructure growth technology provides a great variety of lattice-matched and pseudomorphic AlGaAs/GaAs, InAlAs/InGaAs, InP/InGaAs two-dimensional electron gas (2-DEG) channels for field-effect transistors (HEMTs, PHEMTs) [1-3]. High mobility of confined electrons and other advantages have been successfully exploited for fast operation of 2-DEG channels. On the other hand, the same conditions are favourable for excess microwave noise as demonstrated on ungated biased channels [4]. Eventually, at sufficiently high electric fields, the electrons are heated up, and the hot electrons are liberated from the quantum well [5], this leading to loss of the merit resulting from electron confinement. The hot-electron deconfinement and other hot-electron effects cause onset of new sources of fluctuations absent in 3-DEG channels (for discussion of noise observed in uniformly doped n-type Si, GaAs, InP see [6]). The sources of excess microwave noise in AlGaAs/GaAs-based channels have been recently reviewed [7].

This report considers electronic noise at microwave frequencies resulting from hot-electron velocity fluctuations in an ungated 2-DEG channel when the electrons are heated by the electric field applied along the channel. Origin of the longitudinal fluctuations is discussed in their relation to the fast kinetic processes specific to 2-DEG channels, the processes being excited/quenched by changing electric field, lattice temperature, heterobarrier height, channel length, and doping.

Hot-electron velocity fluctuations due to real space transfer [8] have been resolved in selectively-doped AlGaAs/GaAs channels [9]. The threshold field for this source of noise increases with the increase in the heterobarrier height [10,11]. A special case of real space transfer is transverse tunneling of hot electrons across a thin barrier of AlAs separating the 2-DEG channel and the ionized donors in AlGaAs/GaAs/AlAs/GaAs structure. The related fluctuations of hot electron velocities are resolved, they are heavily suppressed in short channels [12]. Strong thermal quenching of the velocity fluctuations resulting from the real space transfer over the barrier [9] and from the hot-electron tunneling through the barrier [13] is observed.

Enhanced energy loss on acoustic phonons [14,15] in a narrow quantum well of AlGaAs/GaAs channel causes excess noise at electric fields below 100 V/cm at 80 K [9,11]; this intrasubband source is heavily quenched at a higher lattice temperature. The intersubband noise manifests itself in δ-doped GaAs channels [16], where the upper subbands support higher electron mobilities as compared to more confined electronic states of the lower subbands [17]. Dependence of hot-electron noise on the quantum well shape is important in quasi-triangular and quasi-rectangular quantum wells in InGaAs-based 2-DEG channels [18]. These heterostructures can be heavily doped in order to obtain high-density 2-DEG useful for high-power applications. Heavy doping of InAlAs/InGaAs/InAlAs structures is accompanied by the excess fluctuations absent in the low-density 2-DEG channels [19].

2-DEG channels

Figure 1 presents a schematic view of typical MOCVD and MBE grown 2-DEG structures. A V-shaped quantum well is formed in a δ-doped channel located at the donor plane (Fig. 1 a). A single-heterojunction channel (Fig 1 b) contains quasi-triangular quantum well. At equilibrium the electrons are confined at the heterojunction separated from the donor-doped layer. A quasi-rectangular quantum well forms in double-heterojunction channels (Fig. 1 c and d). The well is almost rectangular in case of two-sided doping (Fig. 1 d). A triple-heterojunction channel contains an undoped wide-band-gap barrier inserted between the donor-doped layer and the 2-DEG to prevent deconfinement of the electrons (Fig. 1 e).

a) δ-doped

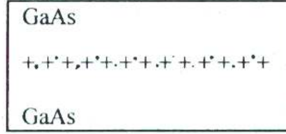

b) selectively-doped single-heterojunction

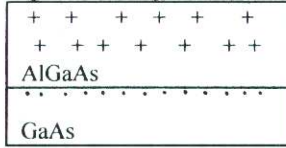

c) δ-doped double-heterojunction

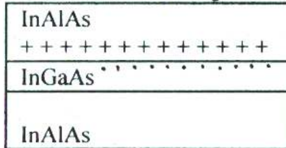

d) twice δ-doped double-heterojunction

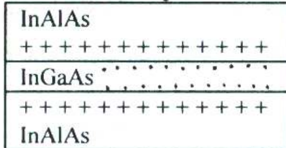

e) δ-doped triple-heterojunction

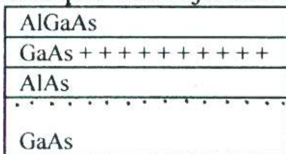

Fig.1. Typical 2-DEG channels.

Experimental

Longitudinal hot-electron velocity fluctuations are investigated in the direction of current flow. Ungated channels supplied with coplanar ohmic electrodes (TLM structures) suit for these purposes. Short-time-domain gated radiometric technique [6] is applied to measure the noise power emitted by the channel into the waveguide. In order to reduce thermal walkout, short pulses of voltage are used. The microwave radiometer is opened for the 0.5-2 μs gating time during the voltage pulse. The equivalent noise temperature T_n is determined from the noise power ΔP_n emitted by the matched channel into the radiometer bandwidth Δf:

$$T_n = \Delta P_n /(k_B\, \Delta f). \qquad (1)$$

The electron number fluctuations do not manifest themselves at microwave frequencies, and the spectral density of electron velocity fluctuations $S_v(E)$ is determined from the spectral density of current fluctuations $S_J(E)$ obtained according to:

$$S_J(E)/S_{J0}= T_n(E)/T_0\; \sigma(E)/\sigma_0 \qquad (2)$$

from the experimental data on the noise temperature and the small-signal conductance σ of the channel. The equilibrium value S_{J0} is available from the low-field data according to Nyquist relation. The equilibrium value $S_{v0} = 4\,(k_BT_0/e)\,\mu_0$., where μ_0 is the low-field mobility. We shall consider the experimental data obtained at 10 GHz frequency unless otherwise stated.

Reversible real space transfer

The experimental data on hot-electron noise temperature for AlGaAs-contained long channels are given in Fig. 2 [10-12]. The noise sources, absent in GaAs, are resolved in 2-DEG channels at electric fields below the threshold for the intervalley transfer noise (the latter dominates in GaAs at fields over 2 kV/cm [6]). The threshold field for the resolved noise in the 2-DEG channels depends on the conduction band offset (see Al mole ratio in Table 1).

Table 1. AlGaAs/GaAs-based channel parameters at 80 K [10-12].

	AlGaAs/GaAs		AlGaAs/GaAs/AlAs/GaAs
Channel	A	B	C
Al mole ratio in the spacer	0.25	0.33	1.0
Spacer thickness, nm	3	40	2.5
Electron density, $10^{11}cm^{-2}$	5.7	1.9	13
Electron mobility, cm^2/Vs	75 000	103 000	35 000

A simple interpretation of the longitudinal hot-electron noise in terms of field-controlled real space transfer of hot electrons can be given for channel B [11]. Fig. 3 illustrates the subband energy spectra calculated by self-consistent solution of coupled Schrödinger-Poisson equations for single-heterojunction AlGaAs/GaAs channels A and B. At equilibrium the electrons occupy the right-hand lower well where the electron mobility is high. The left-hand upper well is empty, unless the electrons are hot and the real space transfer [5] takes place between the undoped GaAs layer and the adjacent doped AlGaAs layer.

A comparison of the noise results (Fig. 2) for channels A and B having different energy separation between the wells (Fig. 3) confirm the natural expectation that the threshold field for the real space transfer should depend on the barrier responsible for the 2-DEG confinement in the lower well. This behavior cannot be accounted for by a higher low-field mobility in channel B (Table 1), since the higher mobility μ_0 leads to a higher power $P = e\mu_0E^2$ received by an average electron from the applied electric field E.

Figure 4 presents the spectral density of hot-electron velocity fluctuations. The maxima of S_v are resolved at the intermediate fields where the spectral density reaches its minimum in bulk GaAs. The position of the maxima depend on the barrier height (cf. Fig. 3), the shape is similar to that obtained by Monte Carlo simulation of the real space transfer [8]. By the way, the intervalley fluctuations of hot electrons dominating in GaAs at field over 2 kV/cm are suppressed by the real space transfer (cf. solid line for GaAs in Fig. 4 and circles and squares), what is confirmed by experimental [9-11] and simulation [8] data.

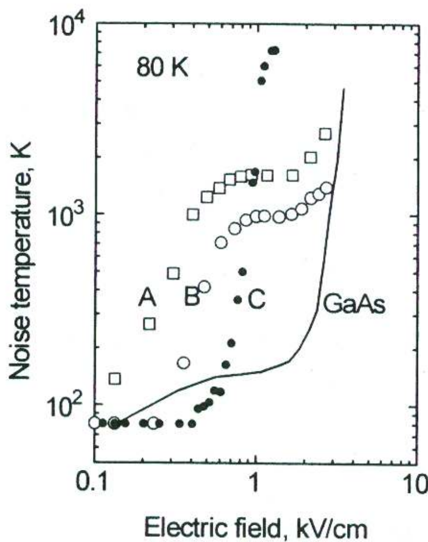

Fig. 2. Noise temperature for AlGaAs based heterostructures with different Al mole ratio in the spacer: A - 25% [10], B - 33%, [11] and C - 100% [12]. Solid line is for GaAs [6].

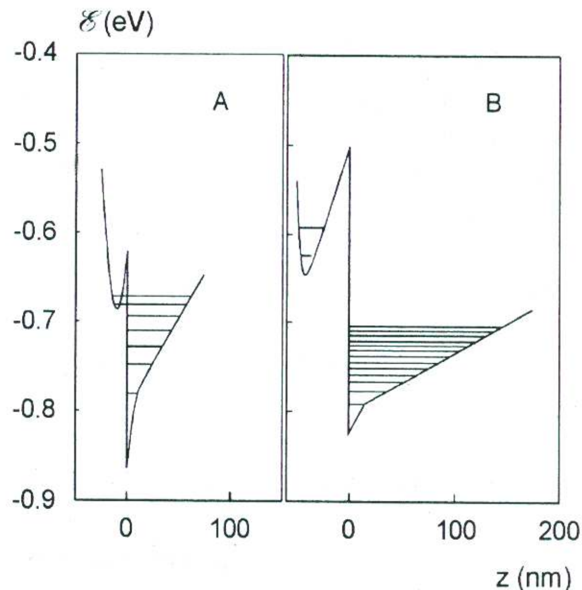

Fig. 3. Subband energy spectra of selectively doped single-heterojunction AlGaAs/GaAs channels A and B (see Table 1). At equilibrium the electrons occupy the right-hand quantum wells located in the undoped GaAs layer [11].

Time constant of reversible real space transfer

By assuming the intrawell processes to be essentially faster as compared to the interwell transfer, the spectral density of velocity fluctuations in the direction of current can be decomposed into:

$$S_v = n_1 S_1 + n_2 S_2 + S_{12}, \qquad (3)$$

where n_1 and n_2 are the normalized partial densities of electrons in the lower and the upper wells under steady state, n_1S_1 and n_2S_2 are the weighted spectral densities of drift velocity fluctuations in the wells neglecting the well coupling, and S_{12} is caused by the partition fluctuations resulting from the interwell transitions.

A simple formula can be applied to discuss the partition fluctuations caused by reversible real space transfer:

$$S_{12} = 4 n_1 n_2 (v_1 - v_2)^2 \tau_{RST}, \qquad (4)$$

where v_1 and v_2 are the drift velocities in the wells, ω is the frequency, and τ_{RST} is the real space transfer time constant

$$\tau_{RST}^{-1} = \tau_{12}^{-1} + \tau_{21}^{-1} \qquad (5)$$

determined by the back-and-forth real space transfer probabilities τ_{12}^{-1} and τ_{21}^{-1}.

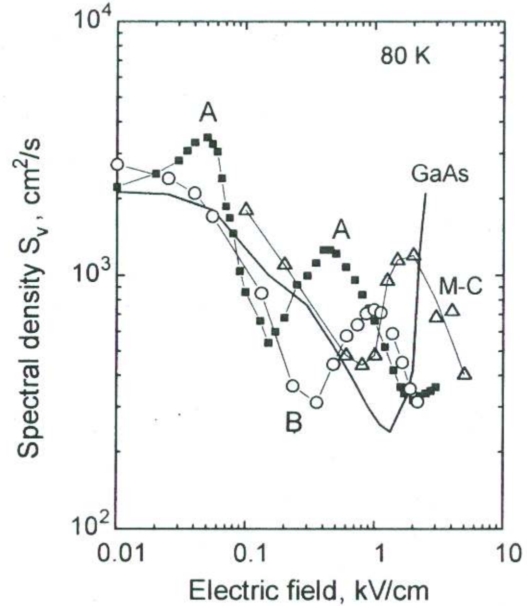

Fig. 4. Field-dependent spectral density of velocity fluctuations for AlGaAs/GaAs channels A and B (squares and circles [10,11]) at 80 K together with results of Monte Carlo simulation (triangles [8]) and GaAs data (solid line [6]). For channel parametres see Table 1.

Eq. (4) shows that the transverse real space transfer contributes to the longitudinal velocity fluctuations provided the electron drift velocities in the wells differ. There is no contribution at thermal equilibrium. A monotonous increase of the electron density ratio n_2/n_1 with an increase of electric field is expected for the nonequivalent wells (Fig. 3). It leads to formation of the maximum of S_{12} at $n_1=n_2$. The related maximum is observed [10] at 1 kV/cm field in channel B (Fig. 4). Under assumption that $v_1 - v_2 \sim 10^7$ cm/s and $n_1=n_2$, the real space transfer time for channel B is estimated according to Eq. (4) with the result: $\tau_{RST} \sim 5$ ps [11]. The obtained time constant being short, the transfer probabilities, τ_{12}^{-1} and τ_{21}^{-1}, should be high at the electric field corresponding to $n_1=n_2$. For the return probability not to be too small, efficient electron heating in the low-mobility well in the doped AlGaAs layer must be assumed [11].

In channel A (Table 1), the wells in the undoped GaAs and the doped AlGaAs are separated by the thin barrier which is transparent for electrons at energies higher than the bottom energy of the upper well (cf. Fig. 3, channel A). The high energy electrons are shared by the two wells, and they are subjected to impurity scattering in the upper well resulting in a lower drift velocity than that of the electrons confined in the lower well. Two groups of electrons with different drift velocities can be introduced, and, after certain modifications, the idea of partition fluctuations remains useful to interpret the maximum of spectral density dominating at the intermediate fields (Fig. 4, closed squares). Independently of the detailed interpretation, the well energy separation decides the range of electric fields for the noise source to manifest itself.

Intrasubband scattering

Channel A (Fig. 4) demonstrates another maximum of the noise temperature in the field range below 100 V/cm. No similar maximum is observed in GaAs and in channel B (Fig. 4). This gives a strong experimental argument that the maximum in question is specific to the narrow well (Fig.3, channel A), while the wide well (Fig. 3, channel B) and GaAs demonstrate monotonous decrease of the fluctuation density in the range of electric fields of interest. The maximum is thought [7] to result from intrasubband scattering of two-dimensional electrons by acoustic phonons. The well breaks translation symmetry, and momentum conservation fails in the direction transverse to the well plane. This results into a wider spectrum of acoustic phonons involved into the scattering events [20]. As a result, acoustic scattering becomes inelastic in narrow quantum wells [14,15].

The enhanced inelasticity of scattering can manifest itself at low temperatures in high mobility channels where acoustic scattering dominates. Figure 5 compares the spectral density of electron velocity fluctuations in a narrow quantum well squares [11]) and in bulk GaAs (solid line [6]). This essentially different behaviour can be explained [7] as follows.

In bulk GaAs, the energy loss by hot electrons is controlled by optical phonons. At low temperatures and not too high electric fields, this energy loss mechanism cause almost periodic motion producing little noise unless disturbed by other scattering events. Acoustic phonon scattering in GaAs does not disturb much, and the fluctuation spectral density tends to decrease upon electron heating (Fig. 5, solid line) together with the decrease of mobility resulting from non-ohmic behaviour of the hot electrons.

The enhanced non-elasticity of acoustic scattering onsets a strong energy loss mechanism responsible for nearly parabolic increase of electron chaotic energy [15]. The optical phonon emission is blocked until the electric field becomes strong enough for the electrons to avoid acoustic scattering. The competition between the acoustic randomization and optical phonon emission shapes the observed maximum of velocity fluctuations (Fig. 5, open squares). The fluctuations at $E < 40$ V/cm can be described in terms of the energy relaxation time τ_ε:

$$S_v = S_{v0} + 4\mu_0^2 E^2 \tau_\varepsilon . \qquad (6)$$

A reasonable fit to the experimental results is obtained with $\tau_\varepsilon = 40$ ps [11] (Fig. 5, dots). Deformation acoustic scattering leads to a longer relaxation time constant, $\tau_\varepsilon = 200$ ps [15], and other scattering mechanisms (piezoelectric acoustic scattering, etc.) are thought to contribute.

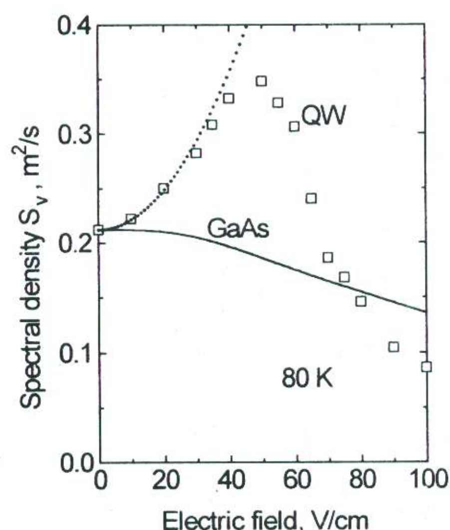

Fig. 5. The spectral density of hot-electron velocity fluctuations for AlGaAs/GaAs channel A (squares [11]) and GaAs (solid line [6]). Dots are Eq. (6).

Thermal effects on real space transfer

Higher lattice temperatures favour electron scattering by optical phonons and make electron heating less efficient. This reduces the probability for an electron to jump over the barrier. Thus the transverse back-and-forth fluxes become balanced at higher electric fields. The experiments confirm the expected changes (Fig. 6) [13]. By the way, the real space transfer fluctuations at 175 K reach the maximum at fields over 3 kV/cm where the intervalley noise dominates in GaAs.

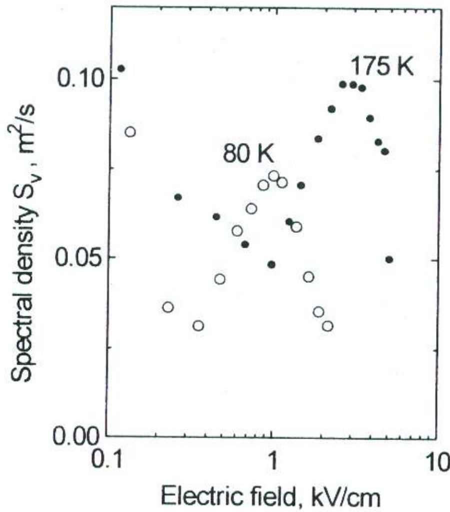

Fig. 6. Field-dependent spectral density of hot-electron velocity fluctuations for single-heterojunction AlGaAs/GaAs channel B (see Table 1) at different lattice temperatures [13].

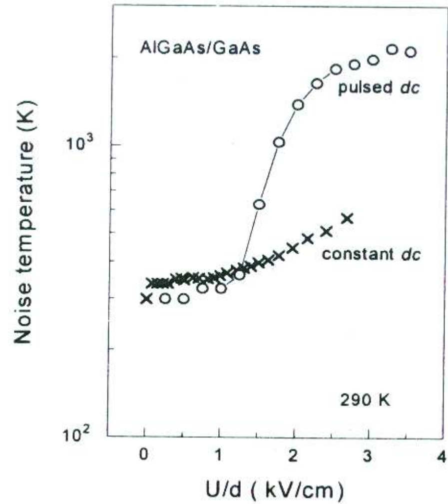

Fig. 7. Noise temperature versus average field for AlGaAs/GaAs channel B (see Table 1) at room temperature: pulsed bias (4 μs, open circles) and constant bias (crosses) [13].

The overlap of the field ranges for the intervalley transfer and the real space transfer makes it difficult to resolve the latter at room temperature [9,13], especially if the thermal walkout due to current flow is not avoided [4,21]. Figure 7 illustrates the interference of the thermal and the electronic processes: the electronic noise due to real space transfer in the 2-DEG channel is strongly quenched by channel overheat resulting from Joule effect under continuous flow of current. For similar results on channel A see [9].

Longitudinal fluctuations due to transverse tunneling

The 2-DEG channel can be separated from the ionized donors by a thin undoped layer of wide-band-gap semiconductor constituting a high barrier for the electrons. A triple-heterojunction AlGaAs/δ-GaAs/AlAs/GaAs structure is designed (Fig.1 e) to have two quantum wells separated by a thin layer of AlAs. Figure 8 presents the results of subband structure calculations; the occupied and the empty wells are treated independently [12]. The electrons are confined the in the lower well at equilibrium.

At fields up to 700 V/cm, the AlGaAs/δ-GaAs/AlAs/GaAs structure (Fig. 2, channel C) demonstrates a lower noise temperature as compared to AlGaAs/GaAs channels containing no AlAs layer [12]. This means that the AlAs barrier is efficient in preventing real space transfer fluctuations in this range of fields. Strong excess noise appears at higher electric fields. Since the barrier is high, the intervalley transfer would take place in GaAs before the electrons would jump ***over*** the barrier. However, the field range where the excess noise dominates is well below the threshold for the intervalley transfer in GaAs. Thus the jumps over the barrier are excluded.

On the other hand, the barrier is thin, and the electrons can penetrate it by tunneling provided energy conservation is satisfied. The energy prerequisite for the tunneling (cf. Fig. 8) is lower than the intervalley separation gap (~0.3 eV in GaAs). Therefore it has been concluded [12] that transverse tunneling is responsible for the steep increase of the hot-electron noise temperature (Fig. 2, channel C) and the maximum of spectral density of velocity fluctuations (Fig. 9, closed circles) resolved at 1 kV/cm field. In the framework of Eq. (4) under assumption v_1-v_2 ~ 2 10^7 cm/s the time constant for the transverse tunneling is estimated to be τ_T ~ 10 ps [12].

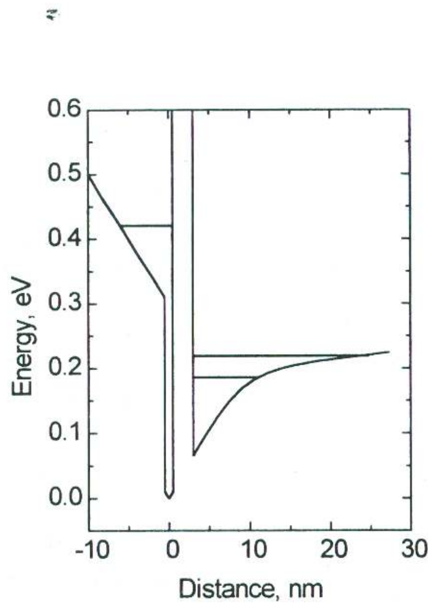

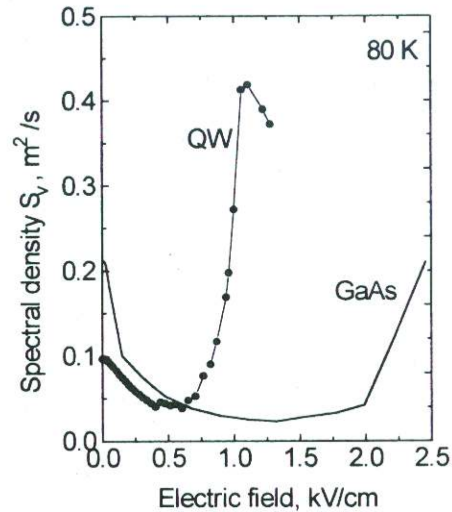

Fig. 8 The lowest subbands in a δ-doped AlGaAs / GaAs / AlAs / GaAs channel, consisting (from right to left) of an undoped GaAs layer, a 2.5 nm undoped AlAs spacer, a 1 nm δ-doped GaAs layer and an undoped AlGaAs layer [12].

Fig. 9. Field-dependent spectral density of electron velocity fluctuations for the AlGaAs /δ-GaAs / AlAs / GaAs channel (closed circles [12]) and bulk GaAs [6]. (Hall effect data for channel C are given in Table 1).

Suppression of tunneling-related noise

The transverse tunneling related noise source (observed in a long channel, Fig. 10, Curve 1) is very weak in the 3 μm channel at fields below 1.5 kV/cm (Curve 2). This strong dependence on channel length can be interpreted in terms of electron transit time t_{tr}. The transit time being short as compared to the tunneling time constant τ_T, the tunneling related fluctuations are eliminated. By assuming for the drift velocity $v = 2 \cdot 10^7$cm/s, one obtains $t_{tr} = 15$ ps.

The tunneling time constants estimated from these two independent experiments are in a reasonably good agreement. Similar results on the tunneling time constant are available from luminescence data for the *resonant* tunneling [24] while the *nonresonant* tunneling time constant is essentially longer [25].

Curves 1 and 3 of Fig. 10 compare the longitudinal noise temperature for the same channel measured at two lattice temperatures. In the field range where the transverse tunneling noise dominates at 80 K, the excess noise is essentially weaker at room temperature. At a fixed electric field say, 1.2 kV/cm, an increase in the lattice temperature leads to the reduction of the longitudinal noise temperature by a factor of 10. This is a nice illustration of the thermal quenching of the hot-electron noise related to the transverse tunneling.

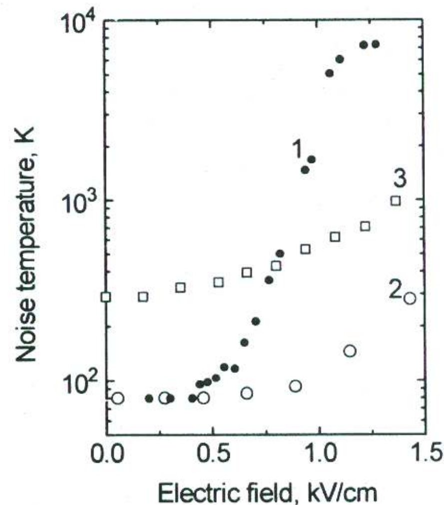

Fig. 10. Hot-electron noise temperature for AlGaAs / δ-GaAs / AlAs / GaAs 2-DEG channels: **1** - 18 μm, 80 K, **2** - 3 μm 80 K [12], **3** - 18 μm, 290 K.

Intersubband scattering

Intersubband scattering can cause excess fluctuations provided electron mobilities in the subbands differ. These partition-type fluctuations, appear in the direction of current. A δ-doped GaAs 2-DEG channel (Fig. 1a) suits for demonstration of the related noise [22,23].

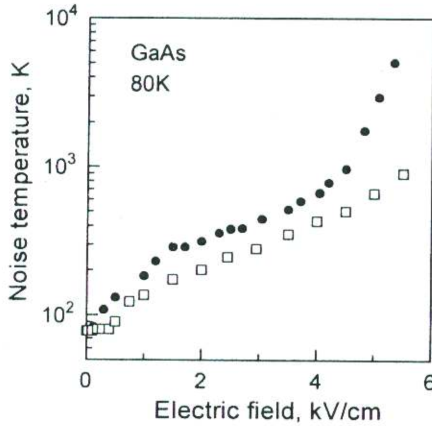

Fig. 11. Hot-electron noise temperature at 80 K for GaAs channels: solid circles stand for the δ-doped 2-DEG channel ($1.5\cdot10^{12}$ cm^{-2} [13]), open squares - for a uniformly doped 3-DEG channel ($3\cdot10^{17}$ cm^{-3} [10]).

Figure 11 presents the experimental results on hot-electron noise temperature for a δ-doped GaAs channel containing $1.5\cdot10^{12}$ cm^{-2} 2-DEG density. The SdH measurements confirm [17] that the electron mobilities in the channel subbands differ essentially: 600 cm^2/Vs in the lowest subband and 3000 cm^2/Vs in the upper one at 1.5 K. The excess noise in the 2-DEG channel is higher as compared to that in a uniformly doped GaAs channel with a similar integral planar density of the electron gas. The noise specific to the 2-DEG channel results from the intersubband fluctuations [13]. Since more than two subbands are involved at high electric fields, a simple two-part partition model (leading to the maximum of S_v, cf. Eq. (5)) does not work in this case.

2-DEG channels on InP substrates

Table 2 presents the Hall effect data for several 2-DEG channels on InP substrates: a selectively δ-doped lattice-matched double-heterojunction InAlAs/InGaAs/InAlAs channel (***I***), a pseudomorphic one with 70 % of Ga in the InGaAs layer (***II***), a twice δ-doped lattice-matched one (***III***), a heavily doped lattice-matched structure containing two 2-DEG channels (***IV***), and a δ-doped lattice-matched AlInAs channel without InGaAs layer (***V***). Relatively low mobility of the electrons in structure ***IV*** (as compared to channel ***I***) results from two-channel conduction: under heavy doping some electrons remain confined in the δ-doped InAlAs layer. The mobility of electrons confined in the δ-doped InAlAs layer is low (Table 2, channel ***V***).

Figure 12 presents the experimental data on noise temperature for channels ***I***, ***II***, and ***III***. Solid line is a parabolic dependence assuming that the excess noise temperature results from the excess kinetic energy $k_B(T_n-T_0) \cong \Delta\varepsilon$, the excess energy $\Delta\varepsilon = e\mu_0E^2\tau_\varepsilon$ being obtained from the balance of energy gain and loss: the power gained from the electric field is $e\mu_0E^2$, the power loss is $\Delta\varepsilon/\tau_\varepsilon$, where τ_ε is the energy relaxation time constant.

Table 2. Electron densities and mobilities for InP-based channels at 300 K and 77 K [18,19].

		300 K		77 K	
Channel	Type	μ (cm^2/Vs)	n (cm^{-2})	μ (cm^2/Vs)	n (cm^{-2})
I	Fig. 1 c, lattice-matched	10600	$2.4\cdot10^{12}$	37000	$2.4\cdot10^{12}$
II	Fig. 1 c, pseudomorphic	11200	$2.3\cdot10^{12}$	37000	$2.4\cdot10^{12}$
III	Fig. 1 d, lattice-matched	7260	$4.1\cdot10^{12}$	37000	$4.3\cdot10^{12}$
IV	Fig. 1 c, lattice-matched	4200	$8.6\cdot10^{12}$	15200	$7.6\cdot10^{12}$
V	δ-InAlAs, Fig. 1a	1200	$9\,6\cdot10^{12}$	2400	$5\cdot10^{12}$

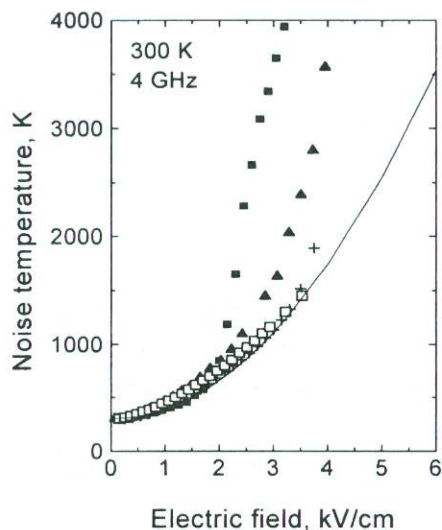

Fig. 12. Hot-electron noise temperature for InP-based 2-DEG channels [18]: solid squares - channel *I* (20 μm), triangles - channel *I* (4.4 μm), crosses - channel *II* (20 μm), open squares - channel *III* (20 μm). Solid line is a fitted parabola.

A reasonable fit of $k_B(T_n-T_0) = e\mu_0 E^2 \tau_\varepsilon$ (Fig. 12, solid line) to the noise temperature data gives an estimate for the energy relaxation time constant: $\tau_\varepsilon \cong 0.7$ ps. The value is close to the momentum relaxation time constant, $\tau_m \cong 0.3$ ps, available from low-field mobility $\mu_0 = (e/m)\ \tau_m$ (see Table 2). This is an argument for the electronic noise dominated by an inelastic scattering, optical phonon emission being the main process [18]. Additional source of noise appears in channel *I* in at fields over 2 kV/cm. This source depends on frequency (cf. Fig. 12 closed squares and Fig. 13 open circles) and channel length (cf. Fig. 12, solid squares and triangles) indicating that a long time constant is involved. The source in question also tends to appear in the pseudomorphic channel *II* at a higher field, especially in 220-800 MHz frequency range. The experimental data (Fig. 12, closed squares and crosses) show a dependence of the threshold field on the conduction band offset, and the related additional source of noise is ascribed to the real space transfer [18]. The frequency dependence, measured in the frequency range from 220 MHz to 10 GHz suggests that the real space transfer time constant is over 100 ps [18]. Channel *III* has donor planes on both sides, its quantum well is close to a rectangular one, and Fermi level is located below that in channel *I*. Only very weak signs of real space transfer noise in the field range below 3 kV/cm are obtained for channel *III* at room temperature [18].

The two-channel structure *IV* is heavily doped, and the 2-DEG channels, similar to channel *I* and channel *V* are contained in it. A steep rise of the noise temperature is observed in channel *IV* at low electric fields turning into nearly-saturated values at the intermediate fields. The noise temperature is essentially higher than that obtained at low/intermediate fields for channel *I* and channel *V*. Thus, data of Fig. 13 give a strong experimental evidence that neither the high-mobility 2-DEG channel *I* nor the low-mobility δ-doped 2DEG channel *V*, nor their weighted combination are sufficient to interpret the noise in channel *IV*, and the partition noise is thought to dominate in the two-channel structure *IV* at low/intermediate fields [19]. A weak dependence of the noise temperature on lattice temperature [19] suggests that electron jumps over the barrier do not participate, and the tunneling of equilibrium electrons is thought to prevail. This is also an illustration that the noise temperature differs from the electron temperature.

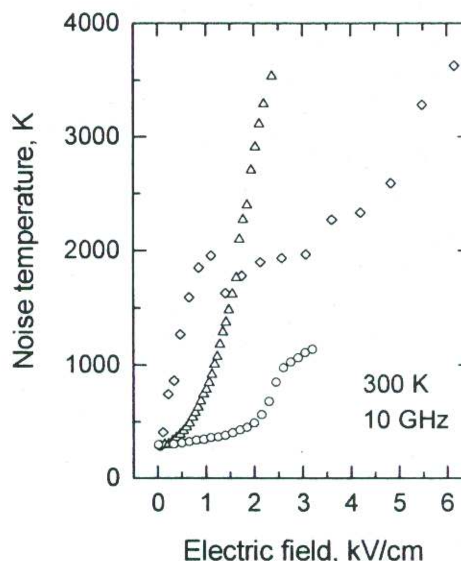

Fig. 13. Noise temperature for InP-based 2-DEG channels [19]: open circles stand for channel *I* (20 μm), diamonds stand for channel *IV* (20 μm), triangles stand for channel *V* (20 μm).

Acknowledgments

The research is supported in part by the Lithuanian State Science and Studies Foundation (P5/94), and the European Commission (ERBCIPDCT 940020, CP 941180)

References

1. S.M.Sze. *High-speed semiconductor devices*. J.Wiley & Sons, 1990.
2. Y.Kwon, D.Pavlidis, T.Brock, and D.Streit. *IEEE Trans. Electron Devices*, **ED42**, 1017 (1995).
3. T.Enoki, K.Arai, A.Kohzen, and Y.Ishii. *IEEE Trans. Electron Devices* **ED42**, 1413 (1995).
4. C.F.Whiteside, G.Bosman, and H.Morkoc. *IEEE Trans. Electron Devices* **ED34**, 2530 (1987).
5. Z.S.Gribnikov, K.Hess, and G.A.Kosinovsky. *J.Appl.Phys.* **77**, 1337 (1995).
6. V.Bareikis, J.Liberis, I.Matulionienė, A.Matulionis, and P.Sakalas. *IEEE Trans. Electron Devices* **ED41**, 2050 (1994).
7. V.Bareikis, R.Katilius, A.Matulionis. In: *Noise in Physical Systems and 1/f Fluctuations*, Proc. 13th Intern. Conf. Eds. V.Bareikis and R.Katilius, World Scientific: Singapore, p.14, 1995.
8. J.Zimmermann, and Y.Wu. *Sol. St. Electron.* **31**, 367-370 (1988).
9. V.Aninkevičius, V.Bareikis, J.Liberis, A.Matulionis, P.S.Kop'ev. In: *Proc. 11th Intern. Conf. Noise in Physical Systems ICNF'91.* Eds. T.Musha, S.Sato, M.Yamamoto, Tokyo: Ohmsha, p.183, 1991.
10. V.Aninkevičius, V.Bareikis, J.Liberis, A.Matulionis, P.Sakalas. *Sol. St. Electron.* **36**, 1339 (1993).
11. V.Aninkevičius, V. Bareikis, R. Katilius, P. S. Kop'ev, M. R. Leys, J. Liberis and A. Matulionis. *Semicond. Sci. Technol.*, **9**, 576 (1994).
12. V.Aninkevičius, V.Bareikis, R.Katilius, J.Liberis, I.Matulionienė, A.Matulionis, P.S.Kop'ev, and V.M.Ustinov. *Solid State Commun.* **98**, 991 (1996).
13. V.Aninkevičius. Dissertation, Vilnius, 1997.
14. V.Karpus. *Fiz.Techn.Poluprov.***20**, 12 (1986).
15. A.Matulionis and C.Jacoboni. In: *Quantum Transport in Ultrasmall Devices*. Eds. D.K.Ferry, H.L.Grubin, C.Jacoboni, A-P. Jauho, Plenum Press, New York, p.453, 1995.
16. V.Aninkevičius, V.Bareikis, R.Katilius, P.M.Koenraad, P.S.Kop'ev, J.Liberis, I.Matulionienė, A.Matulionis, V.M.Ustinov, W.C. van der Vleuten, and J.H.Wolter. In: *Hot Carriers in Semiconductors.* Eds. K.Hess, J-P. Leburton, U.Ravaioli, Plenum Press, New York: 1996, p. 397.
17. P.M.Koenraad. In: *Delta-doping of semiconductors*. Ed. E.F.Schubert. Cambridge University Press, Cambridge, 1996.
18. A.Matulionis, V.Aninkevičius, J.Liberis, I.Matulionienė, J. Berntgen, and D.Gasquet. Report at *Int. Conf. on Noneq. Carrier Dynamics in Semicond. (HCIS-10)*, Berlin, July 28, 1997.
19. V.Aninkevičius, J.Liberis, I.Matulionienė, A.Matulionis, P.Sakalas, B.Henle, E.Kohn, and J.Berntgen. In: *Noise in Physical Systems and 1/f Fluctuations,* Proc. 14th Intern. Conf. Eds. C.Claeys, E.Simoen, World Scientific: Singapore, 1997 (in press).
20. P.J.Price. *Ann.Phys.* **133**, 217-239 (1981).
21. J.Gest, H.Fawaz, H.Kabbaj, and J.Zimmermann. In: *Proc. 11th Int. Conf. Noise in Physical Systems and 1/f Fluctuations ICNF'91,* Ed. T.Musha, Tokyo: Ohmsha, p.291, 1991.
22. V.Bareikis, V.Aninkevičius, J.Liberis, T.Lideikis, A.Matulionis, P.Sakalas, G.Treideris, and R.Katilius. In: *Proc. 1991 Intern. Semicond. Device Research Symposium,* University of Virginia, Charlottesville (USA), p. 469, 1991.
23. V.Bareikis, R.Katilius, A.Matulionis. *AIP Conference Proceedings*, **285**, 181-186 (1993).
24. A.P.Heberle, X.Q.Zhou, A.Tackeuchi, W.W.Rühle, and K.Köhler, *Semicond. Sci. Technol.* **9,** 519 (1994).
25. J.Shah. In: *Hot Carriers in Semiconductor Nanostructures: Physics and Applications.* Ed. J.Shah, Academic Press, San Diego, p.279, 1992.